*Express Polymer Letters Vol.17, No.4 (2023) 373–389*
*Available online at www.expresspolymlett.com*
*https://doi.org/10.3144/expresspolymlett.2023.27*

*Research article*

# Mechanical, thermal and rheological investigation of poly(lactic acid) (PLA)/poly(3-hydroxybutyrate-*co*-hydroxyvalerate) (PHBV) blend within its synergistic elongation effect region

*Hosein Pouriman*[1,2*], *Richard Lin*[1], *Kevin Graham*[2], *Krishnan Jayaraman*[1]

[1]Centre for Advanced Composite Materials, Department of Mechanical and Mechatronics Engineering, The University of Auckland, 1142 Auckland, New Zealand
[2]Friendlypak Ltd Corporation, 51b Rosebank Road, Avondale, 1026 Auckland, New Zealand

*Received 3 July 2022; accepted in revised form 4 November 2022*

**Abstract.** A mathematical Design of Experiments (DOE) was structured to consider the interactive effects of poly(lactic acid) (PLA), poly(3-hydroxybutyrate-*co*-hydroxyvalerate) (PHBV), triethyl citrate (TC) plasticiser, and epoxy functionalised styrene acrylate (ESA) within the synergistic elongational region of the PLA-PHBV blend (PLA/PHBV of 70/30 to 90/10 ratios). Twelve blends were prepared via twin screw extrusion process. Mixture design showed that PLA and TC content has the highest and ESA content has the lowest total effectiveness. The optimal values for the lowest cost and highest elongation at break and the elongational viscosity were reached at PLA/PHBV/plasticiser/ESA content of 0.574/0.3/0.113/0.012 wt%. Rheological studies showed the blends with the highest elongational viscosity were suitable for blown film extrusion.

***Keywords:** biodegradable polymers, polymer blends, and alloys, mechanical properties, PLA-PHBV blend, synergistic elongational effect*

## 1. Introduction

Poly(lactic acid) (PLA) and poly(3-hydroxybutyrate-*co*-hydroxyvalerate) (PHBV) are biodegradable polymers produced from non-petrochemical and sustainable resources with the largest global production amongst biopolymers. PLA is an aliphatic homopolymer produced via ring opening polymerisation of lactide or via polycondensation of lactic acid [1–3]. The methyl side group and the short repeat unit make PLA slow to crystallise and intrinsically a brittle polymer [4]. In addition, PLA has poor impact-energy absorption and barrier properties to aroma, oxygen, and water vapour compared to other widely used thermoplastics for packaging applications [5]. For these reasons, PLA is typically blended with other biopolymers and additives, such as nucleating agents, before processing.

PHBV is the copolymer of polyhydroxy butyrate (PHB) with hydroxy valerate (HV), a subset of polyhydroxyalkanoates (PHAs). In contrast to PLA, which is produced via chemical synthesis, PHAs can be produced from algae or bacteria [6–8]. PHBV has poor tensile strength but excellent gas barrier properties and an impact strength four times greater than PLA [9–12]. Because the mechanical and barrier properties of PLA and PHAs can complement one another, many researchers have investigated the properties and behaviour of PLA/PHA blends at various polymer and additives ratios as a cost-effective method to benefit from the superior properties of each polymer in the

---

[*] Corresponding author, e-mail: mpou994@aucklanduni.ac.nz

blend [13]. One of the caveats of polymer blending is that improving one property could sometimes result in the deterioration of another [14, 15].

Researchers have investigated the PLA-PHBV blend with and without incorporating compatibilisers. In practice, the absence of a compatibiliser results in the break-up, dispersion, and coalescence of the minor polymer phase in the major phase [16–19]. This behaviour is attributed to the low interfacial adhesion between two polymer phases. The in situ reactive extrusion method has improved the miscibility and compatibility between PLA and PHBV [20]. Researchers have reported a synergistic elongational increase in the PLA/PHBV ratio from 70/30 to 95/10 percent [21–24]. This synergistic effect has often been addressed as an unusual blend behaviour that resulted in elongational increases up to 1056% (from 4.8 to 50.7%) [21].

Among the literature, Zhao *et al*. [24] reported an increase of about 250% in the strain at the break at the PLA/PHBV ratio of 85/15 and about 50% at the PLA/PHBV ratio of 70/30 compared to pristine PLA. Noda *et al*. [25] reported that the addition of 10 wt% PHA to PLA increased the elongation of the blend by 100% and attributed this behaviour to the presence of the amorphous phase in the blend. They further discuss that the deformation mechanism is different within this region compared to the rest of the blend ratio. The failure points are localised without propagating to sudden sample failure. Nanda *et al*. [26] found a 110 and 250% increase in elongation at break at PLA/PHBV 60/40 and 70/30, respectively. Although the biggest elongational increase happened in the synergistic region, the elongation at break of all samples processed at the same screw speed (150 rpm) was reported to be higher than that of the pristine polymers. In another study, Ma *et al*. [23] found that the incorporation of 10 to 30% PHBV into PLA significantly increased the ductility of PLA. They report that at the PLA/PHBV ratio of 80/20, the increase of elongation at break is 5750% (from 4 to 230%). Han *et al*. [27] also blended 5 to 30% PHBV with PLA and reported a 317% increase of elongation at break in PLA/PHBV 80/20. This value is 57 times greater than that of PLA. And again, with the linear increase of PHBV content in the blend, the elongation at break decreased. Gérard *et al*. [21] reports similar results and an increase of 204 and 50.7% at the 90/10 and 80/20 ratios, respectively. Liu *et al*. [28] also noticed the elongation increase in the 70/30 to 90/10 region, with the 80/20 having a 500% increase compared to pure PLA. In more recent studies, researchers have incorporated PLA and PHBV with other polymers and additives [29–31], which makes the synergistic region non-conclusive to the effect of PLA and PHBV polymers only. However, an outlier elongational increase at high PLA content can be seen. The decrease in tensile strength due to the addition of PHBV content within the synergistic elongational region of the PLA-PHBV blend reported in the literature is between 5 to 10% compared to pristine PLA [26, 32].

The elongational increase and relative tensile strength stability within the synergistic region promise further investigation, specifically for flexible packaging applications. At the time of writing this paper, we have not found any journal article specifically investigating the synergistic elongational region in PLA/PHBV blend with a systematic ‘Design of Experiments approach. In this research, a mixture design has been defined within the PLA/PHBV ratio of 70/30 to 90/10 to count for the interactive effect of each blend component. A plasticiser and epoxy functionalised styrene acrylate (ESA) chain extender were added to the blend to enhance the elongation at break further and improve the melt strength.

## 2. Materials and methodology

### 2.1. Materials

To improve the miscibility of PLA and PHBV, the polymer grades with a minimum difference between their melting temperatures were selected. For PLA, Ingeo™ Biopolymer 2003D (melt flow rate (MFR), 6 g/10 min, 210 °C, 2.16 kg) with $T_m = 160$ °C was supplied from NatureWorks (Minnesota, USA). For PHBV polymer, ENMAT™ Thermoplastics Resin Y1000P (MFR = 8–15 g/10 min, 180 °C, 2.16 kg) was supplied from TianAn Biopolymer (Ningbo, China). For the ESA chain extender, Joncryl ADR 4468 was provided by BASF, Singapore. Triethyl citrate (TC) plasticiser ($C_{12}H_{20}O_7$) with a molecular weight of 276.28 g/mol (CAS-No 77-93-0) was supplied by Sigma Aldrich (Milwaukee, USA). All materials were consumed as received.

### 2.2. Methodology

The candidate batches to proceed further to blown film extrusion were chosen based on exhibiting the highest values of elongational viscosity and elongational strain.

As mentioned earlier, a synergistic effect between the blend constituents at PLA/PHBV ratios of 70/30 to 90/10 is expected; hence the mixture design statistical analysis was employed to analyse the interactive effects of each mixture component on different properties of the blends. Mixture design is typically utilised when the only intended variable in the manufacturing of one mixture is the content ratio of its constituent, and other factors that could contribute to the manufacturing, *e.g.*, process temperature, process time, etc., remain unchanged. Hence in mixture design, responses only depend on the relative proportion of components. Minitab software was used to generate the material proportions of all testing batches (Table 1).

Twelve different batches were manufactured based on mixture design. In addition, three batches with pristine PLA to PHBV ratios of 70/30, 80/20, and 90/10 (A70, A80, A90) with no plasticiser and chain extender were manufactured to draw a comparison with other samples containing plasticiser and chain extender. Extreme vertices design was chosen with a linear constraint of 0.82 < PLA + PHBV < 0.95 and quadratic model type. In quadratic models, if, for example, A, B, and mixture components, the model will calculate the linear as well as the AB, AC, and BC relationships. Extreme vertices of the constraint design space using the XVERT algorithm were generated, as shown in Figure 1. Using Piepel's CONAEV algorithm, the centroid points can be calculated up to the specified degree.

**Table 1.** The weight percent materials of testing batches based on mixture design.

| | Weight percent of component | | | |
|---|---|---|---|---|
| **Batch** | **PLA** | **PHBV** | **Triethyl citrate** | **ESA** |
| 1 | 83.8 | 8.2 | 5.0 | 3.0 |
| 2 | 76.8 | 8.2 | 15.0 | 0.0 |
| 3 | 73.8 | 8.2 | 15.0 | 3.0 |
| 4 | 66.5 | 28.5 | 5.0 | 0 |
| 5 | 63.5 | 28.5 | 5.0 | 3.0 |
| 6 | 85.5 | 8.2 | 5.0 | 1.3 |
| 7 | 85.5 | 8.2 | 6.3 | 0 |
| 8 | 85.5 | 9.5 | 5.0 | 0 |
| 9 | 57.4 | 28.5 | 14.1 | 0 |
| 10 | 57.4 | 27.6 | 15.0 | 0 |
| 11 | 57.4 | 28.5 | 11.1 | 3.0 |
| 12 | 57.4 | 24.6 | 15.0 | 3.0 |
| A70 | 70.0 | 30.0 | 0 | 0 |
| A80 | 80.0 | 20.0 | 0 | 0 |
| A90 | 90.0 | 10.0 | 0 | 0 |

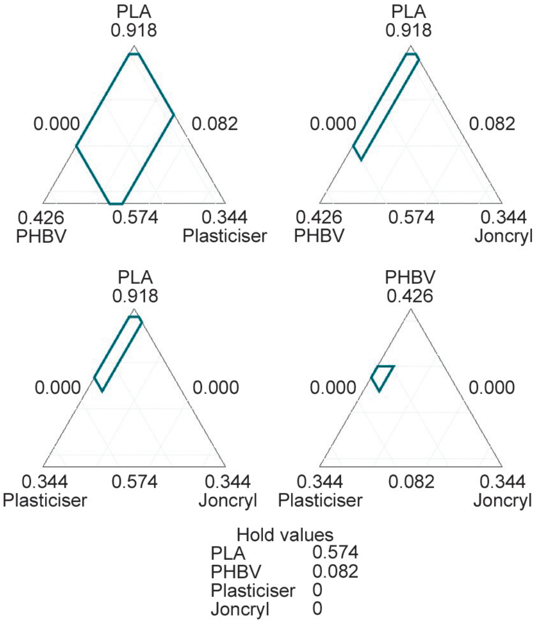

**Figure 1.** Matrix of simplex design plots in amounts.

The Cox response trace plots were used to examine the effect of each component on the response. The trace curves depict the impact of changing a component's value along an imaginary line connecting the reference blend and the vertex. The following were considered when interpreting the response trace plots:

- The steeper the response traces, the greater the effect on the response.
- Components were analysed relative to the reference mixture.
- Longer response traces are indicative of the components with larger widths (upper and lower bounds), and shorter response traces are indicative of the components with the smaller width.
- The total influence of a component is determined by the component's range as well as the steepness of its response trace.
- The total influence is determined by the difference in response between where the effect direction point in the component is at its lower bound and the effect direction point where the component is at its upper bound.
- Components with response traces that are nearly horizontal have almost no effect on the response.
- Components that have similar response traces have a similar impact on the specified response.

In this analysis, all residuals were standardised. A residual is a difference between a fitted value ($\hat{y}$) and its corresponding observed value ($y$); in other words, it identifies how accurately a model describes the variance in the observed data. To obtain the standardised residual, the value of the residual was divided by the estimation of its standard deviation. The standardised residuals less than –2 or greater than 2 are generally considered large.

### 2.2.1 Sample manufacturing

*Extruding filaments*

Virgin PLA and PHBV pellets were dried at 90 °C for 3 hours, and the moisture content was recorded to be less than 0.025% (250 ppm). PLA, PHBV, and ESA proportions were premixed and fed to the extruder through the hopper section. TC was proportionally and continuously fed to the extruder through a tube attached to a multi-syringe-equipped liquid pump (Cole-Parmer, IL, USA) equipped with a 60 ml syringe. Each batch was extruded via a co-rotating twin screw extruder (Brabender, Duisburg, Germany) with an *L*/*D* ratio of 40:1, screw diameter of 25 mm, a rotation speed of 75 rpm (delivering a varying torque of 9.5 to 10 N·m) and a temperature profile of 160–180–185–190–185–180 °C from feeding to metering zone and utilising a 4-mm die. The extrudates that were in the form of filaments were cooled down via a downstream air-cooling line and then wound to a filament spool. For further mechanical characterisation, samples of adequate lengths were separated in filament form. The rest of the filaments were pelletised via a pelletiser (Labtech, Samut Prakan, Thailand) to produce samples for rheological studies.

### 2.2.2. Rheology studies

The rheological behaviour of manufactured batches was studied via a dual-barrel capillary rheometer (Rheo-Tester 2000, Göttfert, Buchen, Germany). An isothermal test was conducted at 180 °C with varying apparent shear rates of 100, 200, 500, 1000, 2000, 5000, 6000, and 9000 $s^{-1}$. Barrels were equipped with two capillary dies with 30 and 10 mm lengths and an equal hole diameter of 1 mm. Two pressure transducers capable of 500 and 1000 bar read the die pressures during the test, and the results were recorded by Göttfert's proprietary software WinRheo in real time. Each batch was tested twice, and the results were averaged.

Apparent shear stress ($\tau_a$) was calculated based on Equation (1), where $R$ is the radius of the capillary, $L$ is the capillary 1 length (30 mm), and $P_1$ and $P_2$ are the pressure readings from capillary 1 (30 mm) and capillary 2 (10 mm), respectively:

$$\tau_a = \frac{P_1}{2\frac{L}{R}} \tag{1}$$

By dividing the apparent shear stress by the apparent shear rate ($\gamma_a$), the apparent viscosity ($\eta_a$) can also be calculated [33] (Equation (2)):

$$\eta_a = \frac{\tau_a}{\gamma_a} \tag{2}$$

Based on Bagley correction [34], the corrected shear stress can be calculated as shown in Equation (3):

$$\tau_w = \frac{P_1 - P_2}{2\frac{L}{R}} \tag{3}$$

The Rabinowitsch correction was then used to account for the effect of the non-Newtonian behaviour of molten polymers in the corrected shear rates. Based on this correction, a power-law correlation between $\gamma_a$ and $\tau_w$ (Equation (4)) is drawn. The pseudo plasticity index ($n$) can then be determined as the slope of a double logarithmic plot of $\tau_w$ *versus* $\gamma_a$ (Equation (4)):

$$\tau_w = k\dot{\gamma}_a^n \tag{4}$$

The Rabinowitsch correction can then be incorporated into values of $\gamma_a$, and then the true shear rate ($\dot{\gamma}_w$) can be calculated as in Equation (5), and the true viscosity ($\eta_w$) as in Equation (6):

$$\dot{\gamma}_w = \dot{\gamma}_a \frac{3n+1}{4n} \tag{5}$$

$$\eta_w = \frac{\tau_w}{\dot{\gamma}_w} \tag{6}$$

The Cogswell Equations, Equations (7), (8), and (9), were used to calculate the elongational viscosity of the manufactured batches [35]:

$$\sigma_E = \frac{3}{8}(n+1)P_2 \tag{7}$$

$$\dot{\varepsilon} = \frac{4}{3}\frac{\eta_a \dot{\gamma}_a^2}{(n+1)P_2} \tag{8}$$

$$\eta_e = \frac{\sigma_E}{\dot{\varepsilon}} \tag{9}$$

where $\sigma_E$ denotes the average extensional stress, and the extensional viscosity ($\eta_e$) was calculated via extensional strain ($\dot{\varepsilon}$).

### 2.2.3. Differential scanning calorimetry (DSC)

Thermal analysis was conducted via a differential scanning calorimeter (Q1000™, TA Instruments, DE, USA) at standard mode with a heat/cool/heat cycle. The temperature profile was programmed to cover –50 to 200 °C, with the starting temperature of ambient temperature, heating and cooling rate of 20 K/min, and nitrogen gas purging rate of 50 ml/min. Perforated aluminium pans were used to rid the samples of possible trapped moisture in the first heating cycle. All samples have equal weights of 10±0.1 mg. The melting temperature ($T_m$), glass transition temperature ($T_g$), the onset of crystallisation temperature, and the enthalpy of fusion from recorded thermographs were calculated via the DSC's proprietary software.

### 2.2.4. Mechanical properties characterisation

*Tensile strength and elongation at break*

Tensile strength and elongation at break tests were conducted via a universal tensile testing machine (Instron 5567, Instron, Massachusetts, USA). Single-bollard-type grips were used to hold the filament samples in place. The gauge length of all samples was set to 5 mm and the crosshead speed to 50 mm/min. The gauge length increment was measured and recorded via a high-precision camera. The tensile strength measurements were automatically calculated via Bluhill software, proprietary software for Instron, by reading directly from the testing machine. At least five specimens were tested for each testing sample, and the results were averaged.

## 3. Results and discussion

### 3.1. Mathematical model analysis

The measured results for tensile stress, elongation at break, glass transition temperature, and enthalpy of fusion are presented in Table 2. To determine the accuracy of the models and whether the regression assumptions are met, the plot of residuals vs percent, fitted value, frequency, and observation order was drawn. Probing the residual plots can determine whether the ordinary least square assumptions are met. If these assumptions are met, unbiased coefficient estimates with a minimum difference are produced by the ordinary least square regression. Residual plots are shown in Figures 2 to 5.

The generated fitted values for tensile stress, elongation at break, glass transition temperature, and the onset of crystallisation temperature versus the deviation from reference blend in proportion are depicted in Figure 6. Before individual analysis of each

**Table 2.** Results from mechanical properties tests, thermal analysis, and cost estimation for mathematical model analysis.

| Sample name | PLA | PHBV | Plasticiser | ESA | Cost [NZD/kg] | $\sigma_u$ [MPa] | $\sigma_b$ [MPa] | ε [%] | $T_g$ [°C] | $T_c$ [°C] | $T_m$ [°C] | $\Delta H_{fus}$ [J/g] |
|---|---|---|---|---|---|---|---|---|---|---|---|---|
| 1 | 0.838 | 0.082 | 0.050 | 0.030 | 10.2 | 46.80 | 35.8 | 54 | 50.67 | 51.28 | 142.5 | 16.68 |
| 2 | 0.768 | 0.082 | 0.150 | 0 | 13.4 | 33.70 | 29.1 | 196 | 39.61 | 44.68 | 140.4 | 21.86 |
| 3 | 0.738 | 0.082 | 0.150 | 0.030 | 14.6 | 5.44 | 5.0 | 190 | 36.26 | 43.62 | 135.1 | 35.47 |
| 4 | 0.665 | 0.285 | 0.050 | 0 | 10.3 | 45.90 | 41.6 | 53 | 53.21 | 53.01 | 171.6 | 31.52 |
| 5 | 0.635 | 0.285 | 0.050 | 0.030 | 11.5 | 44.30 | 36.5 | 164 | 48.07 | 52.32 | 167.5 | 29.23 |
| 6 | 0.855 | 0.082 | 0.050 | 0.013 | 9.5 | 45.70 | 32.9 | 113 | 51.08 | 54.61 | 142.9 | 20.06 |
| 7 | 0.855 | 0.082 | 0.063 | 0 | 9.5 | 38.60 | 29.3 | 135 | 51.16 | 52.98 | 144.5 | 12.84 |
| 8 | 0.855 | 0.095 | 0.050 | 0 | 9.1 | 52.10 | 38.2 | 52 | 53.03 | 54.69 | 168.4 | 13.70 |
| 9 | 0.574 | 0.285 | 0.141 | 0 | 14.3 | 34.30 | 34.0 | 189 | 38.05 | 45.90 | 165.1 | 31.74 |
| 10 | 0.574 | 0.276 | 0.150 | 0 | 14.6 | 34.20 | 33.8 | 199 | 38.34 | 42.98 | 167.2 | 33.10 |
| 11 | 0.574 | 0.285 | 0.111 | 0.030 | 14.2 | 34.70 | 31.2 | 206 | 43.79 | 45.66 | 167.0 | 30.66 |
| 12 | 0.574 | 0.246 | 0.150 | 0.030 | 15.6 | 27.40 | 27.1 | 197 | 40.15 | 43.54 | 165.4 | 33.73 |
| 13/A70 | 0.700 | 0.300 | 0 | 0 | 8.2 | 45.90 | 42.7 | 52 | 60.5 | 60.17 | 171.9 | 26.04 |
| 14/A80 | 0.800 | 0.200 | 0 | 0 | 7.6 | 52.50 | 51.5 | 54 | 59.85 | 60.95 | 170.5 | 21.66 |
| 15/A90 | 0.900 | 0.100 | 0 | 0 | 6.99 | 49.60 | 49.3 | 51 | 59.95 | 60.87 | 149.7 | 12.80 |

| | |
|---|---|
| $\sigma_u$ | is the ultimate tensile stress, |
| $\sigma_b$ | is the tensile stress at the break, |
| ε | is the elongation at the break, |
| $T_g$ | is the glass transition temperature, |
| $T_c$ | is the onset of cold crystallisation temperature, |
| $T_m$ | is the temperature at the melting point, |
| $\Delta H_{fus}$ | is the enthalpy of fusion |

response, a common trend that could be identified among all responses is that PLA and TC components have the longest response range (upper and lower bounds); therefore, the highest total effectiveness, and ESA has the shortest range, hence the lowest total effectiveness. The total efficiency of PLA relative to other components is high with respect to its range and steepness, albeit the PLA graph isn't the steepest one in any of the responses. TC for the specified responses may be the most effective component in the blend

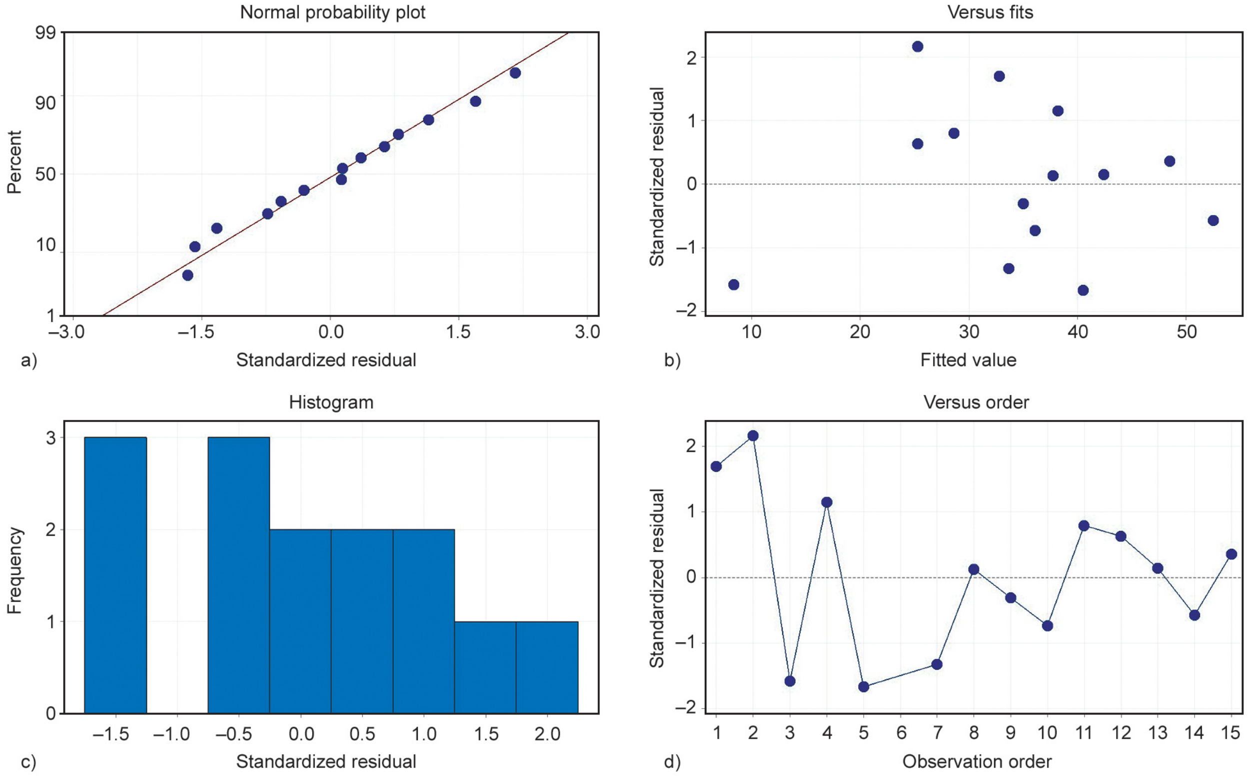

**Figure 2.** Residual plots for tensile stress at break. a) Normal probability plot, b) *versus* fits, c) histogram, d) *versus* order.

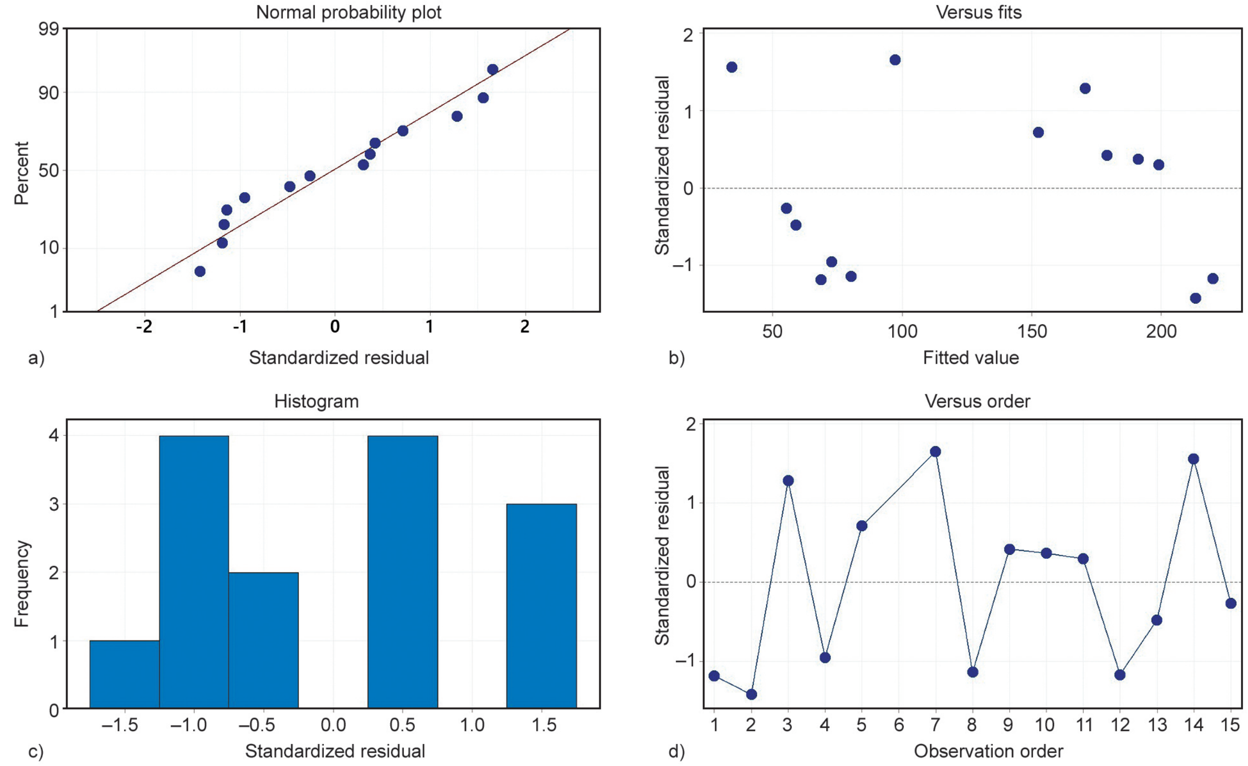

**Figure 3.** Residual plots for elongation at break. a) Normal probability plot, b) *versus* fits, c) histogram, d) *versus* order.

due to its steep presence in all response graphs and an extended range of upper and lower bounds.

It can be seen from the tensile stress response plot (Figure 6a) that PLA and PHBV have a similar response trace but at a different range. With the proportional increase of these components, the tensile stress increases and then decreases. PHBV with a steeper presence denotes higher effectiveness among

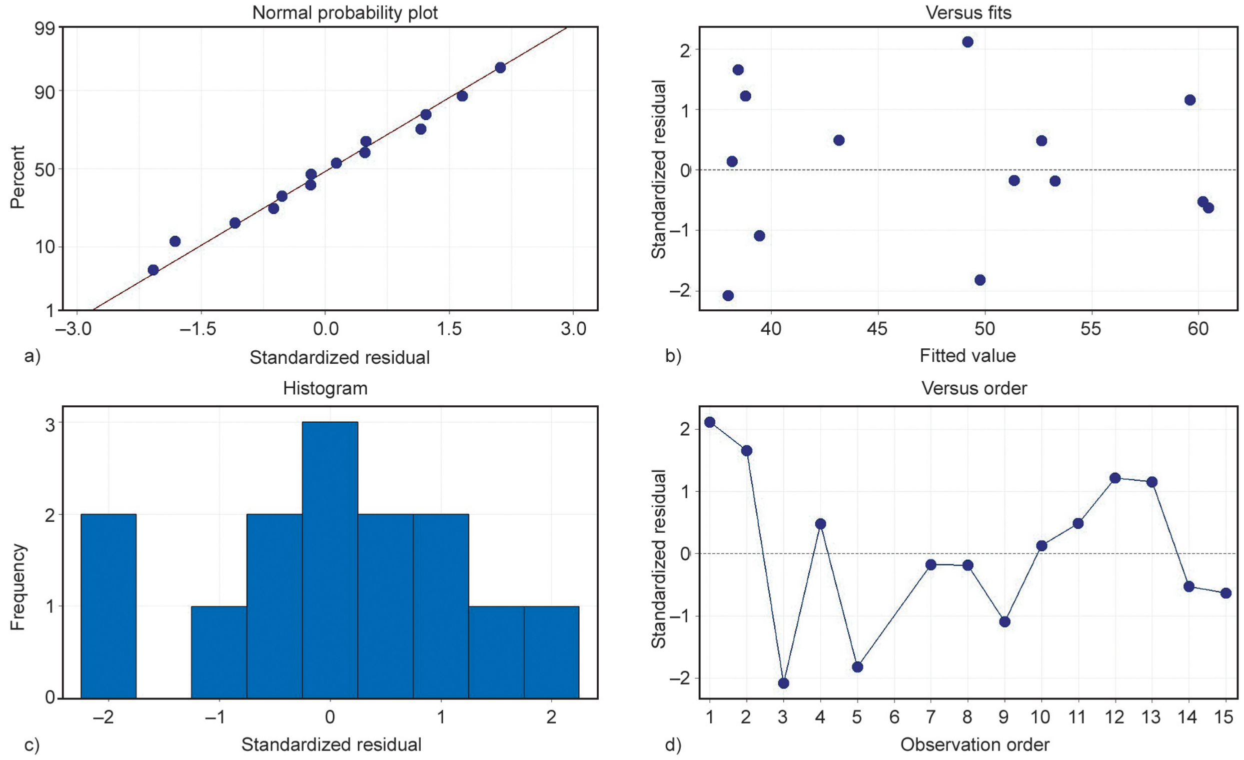

**Figure 4.** Residual plots for glass transition temperature. a) Normal probability plot, b) *versus* fits, c) histogram, d) *versus* order.

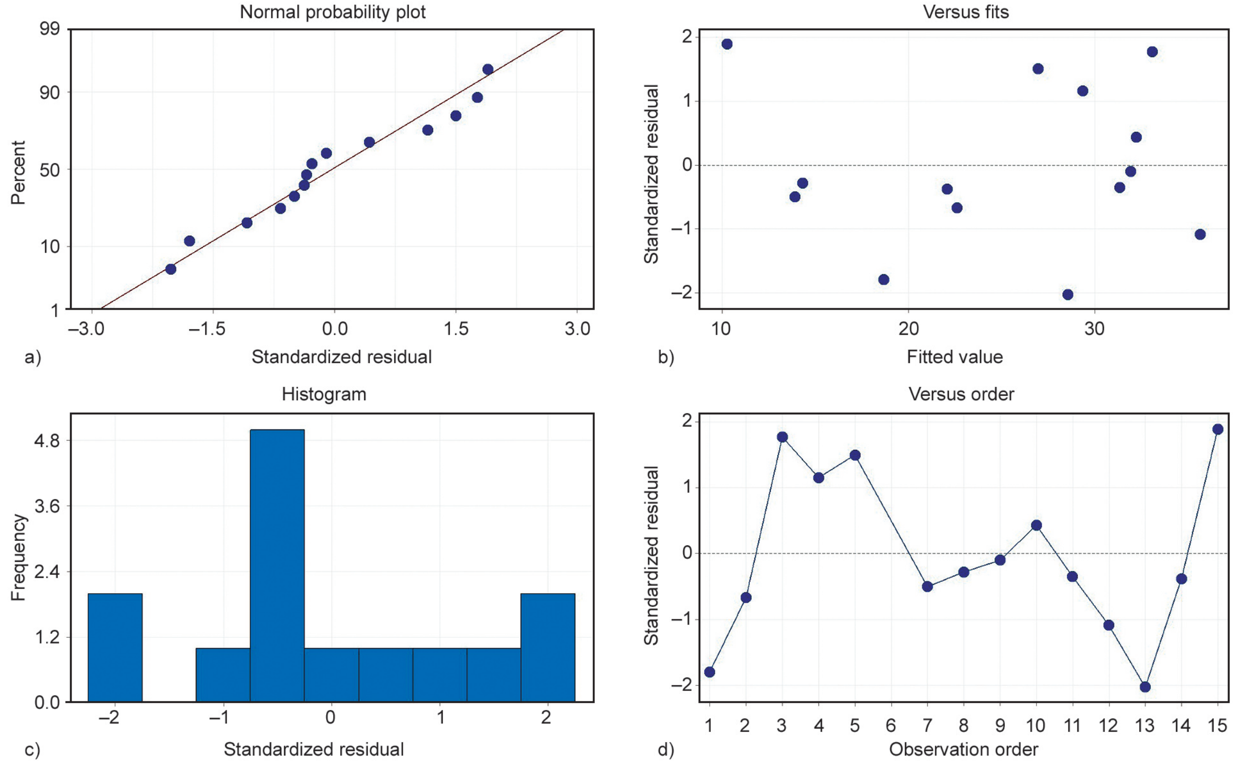

**Figure 5.** Residual plots for enthalpy of fusion. a) Normal probability plot, b) *versus* fits, c) histogram, d) *versus* order.

the two thermoplastics but at a lower range. The TC plasticiser with the steepest line among all components indicates a continuous decline in tensile stress with its proportional addition to the blend. This behaviour can be explained by the function of most plasticisers in the polymer blend. TC molecules with low vapour pressure and molecular weight place themselves among polymer molecules, providing a lubricating effect between polymer chains. This leads to an increase in chain mobility, hence facilitating molecular separation at higher stress loads. The ESA chain extender's low range and short upper and lower bounds indicate its low total effectiveness. The increase of ESA content proportional to other blend components slightly decreases and then increases the tensile stress. ESA chain extender is used in trace contents in the mixture and here shows, it does not have a significant interactive effect with other components in terms of tensile stress.

As shown in Figure 6b, PLA has the longest response trace for the elongation at break response. The proportional increase of PLA content in the blend leads to a rapid and almost linear decrease of the elongational strain of the samples from around 220 to 100%. The high brittleness of PLA can explain this direct correlation between PLA content and elongational strain. In contrast, as expected, the addition of TC led to a linear increase of elongational strain in the samples indicating a non-interactive effect of plasticiser with respect to the increase of other blend components. PHBV and ESA content show a reversed interactive effect on the blend. An increase in PHBV slightly decreases the elongational strain from 140 to 120% and then back to about 150%. PHBV has the lowest response range and the most temperate slope between all components. This indicates that PHBV content is not a significant contributor but has a synergistic effect on the elongational

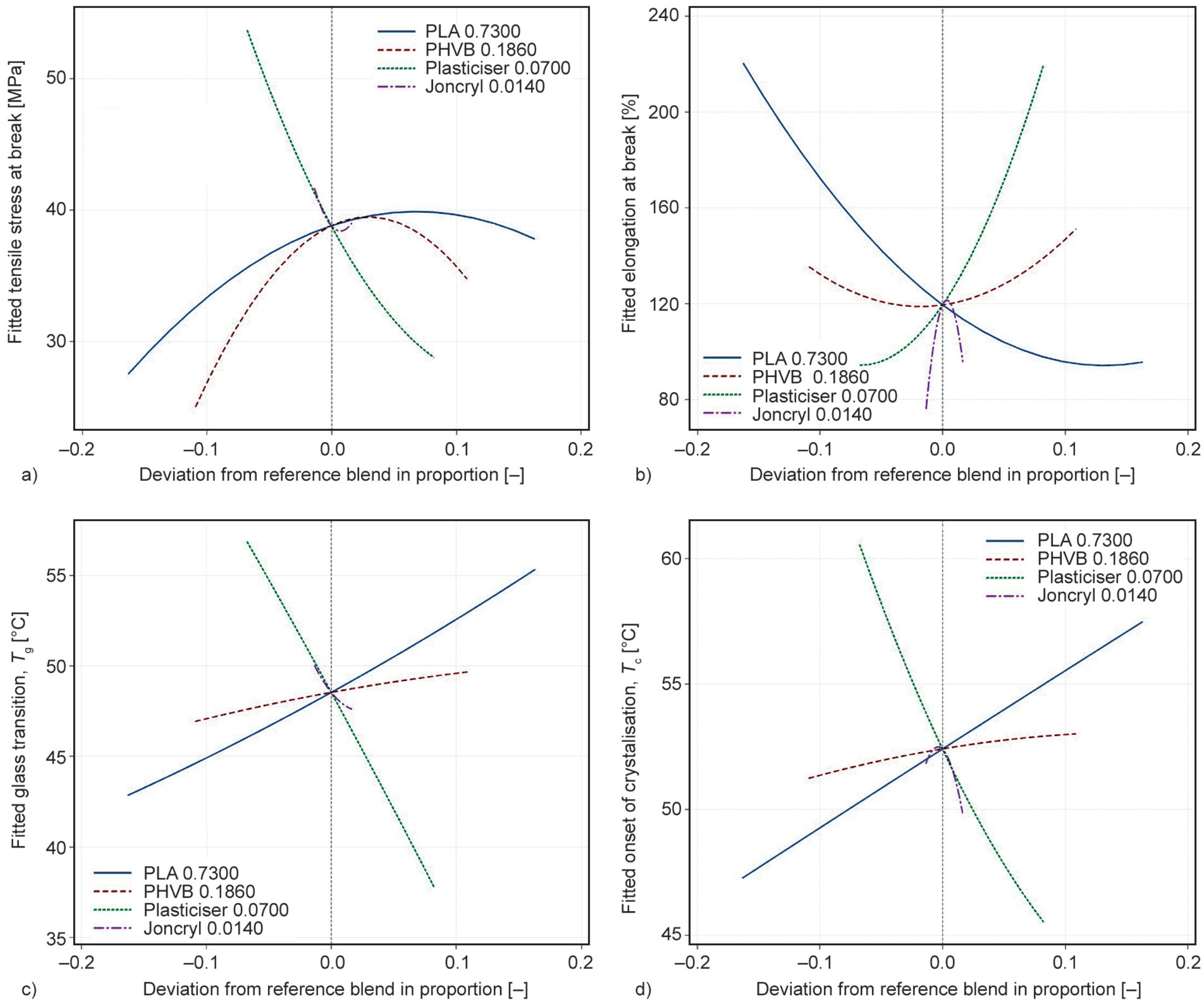

**Figure 6.** Cox response trace plots for a) tensile stress at break, b) elongation at break, c) glass transition temperature and d) the onset of crystallisation.

strain of the compound. ESA content with high effectiveness (steep trace line) at a short response range has a counter effect with PHBV content. It initially increases the strain rate from 80 to 120% at a rapid rate and then declines. These interactive effects justify the importance of mixture design analysis and call for an optimisation study when different properties are to be reached simultaneously.

For the glass transition temperature (Figure 6c), all components show an almost linear response trace signifying a direct relationship with their proportional content increase. The increase of PLA and PHBV contents leads to an increase in the $T_g$. However, PLA has a more significant effect where the effect of PHBV is subdued. The direct correlation between the increase in TC content and the decrease of $T_g$ can be explained as the main functionality of plasticisers in polymer blends, which is to place itself between polymer chains. This affects the intensity of the secondary bonding forces between the polymer chains, decreasing the glass transition temperature, among other effects. ESA chain extender, albeit with low total effectiveness, acts as a plasticiser in glass transition temperature response.

The response trace graphs from the onset of crystallisation temperature ($T_c$) (Figure 6d) are closely similar to the $T_g$ graphs except for the chain extender content. The increase of ESA content shows an interactive effect in the blend with a sudden rise and fall of $T_c$. Although, in this case, the effect of the chain extender is not significant compared to the total effectiveness of other contributors, it can be concluded that ESA could be used in optimum contents to have a maximised $T_c$ response.

The matrixes of cost per material of components were visualised by drawing surface response plots for the main contributing components, as presented in Figure 7. ESA chain extender was omitted from the plots due to its trivial contribution to the overall cost. In surface plots, the mixture components are represented in x and y-axes, the cost on z-axes, and the response on the meshed surface. Overall, it can be concluded that the cost of manufacturing the range of these mixture compositions is highly dependent on the price of PLA and, after that, PHBV, then the plasticiser. This conclusion could change based on the selection of different grades of materials, the year of production, and the market price.

Multiple variables often must be considered when a compound is designed for a real-time application. For this study, the optimisation goals were to lower the cost and increase the elongation at break and the apparent elongational viscosity. The weight and importance of responses were equally distributed. The

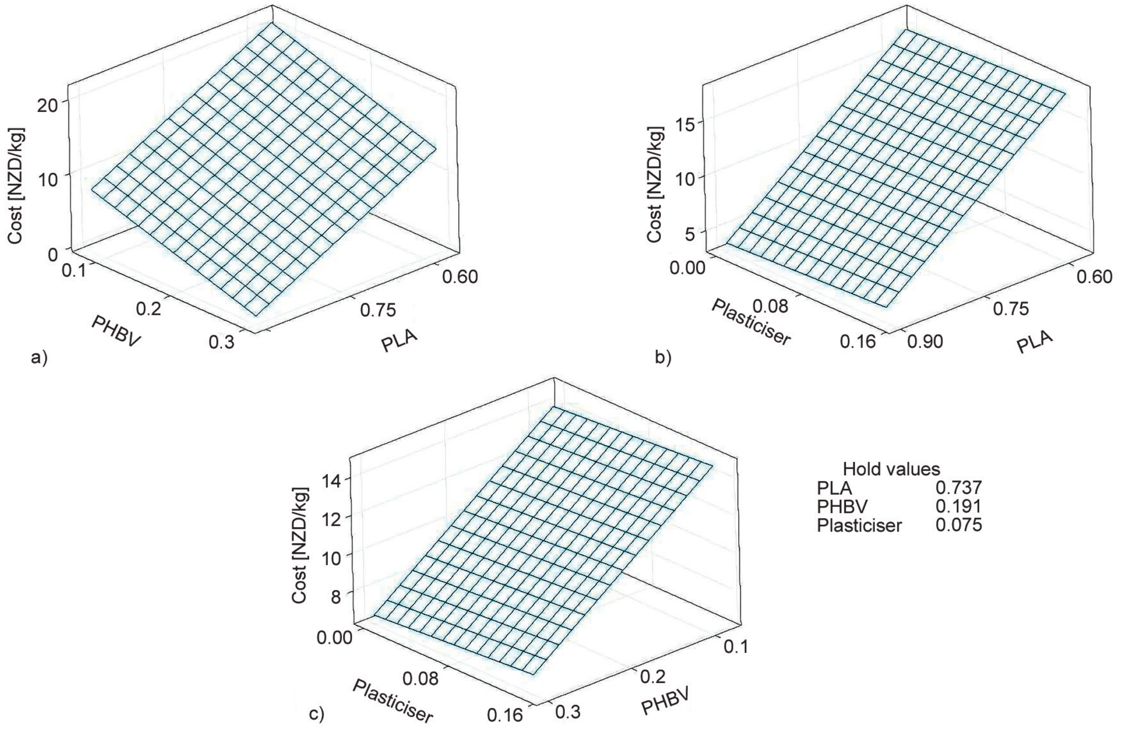

**Figure 7.** Matrix of surface response plots for the cost [NZD/kg] for a) PHBV-PLA, b) plasticiser-PLA and c) plasticiser-PHBV

collected experimental results were used for sensitivity analysis to find the optimal responses and compound values. The goal, the target, and the lower and the higher values of the mentioned properties are presented in Table 3. The tensile stress values were omitted from the optimisation because the tensile stress results were within the desired range.

Individual desirability was calculated for each response. The optimal values were generated when the maximum composite desirability of 0.363988 was reached. The optimal calculated component content and the predicted responses are presented in Table 4. The results of embedding these values in the response optimisation plot are shown in Figure 8. Red vertical lines represent optimal compositions. One can control how the changes affect the response by adjusting the variable settings.

## 3.2. Mechanical properties

The yield stress, ultimate tensile stress, and tensile stress at break follow almost a similar trend from one sample to another, which is quite different from the strain at break. These two results were separated into different figures, as presented in Figure 9 and Figure 10. The deepest dive in the tensile properties among samples happen as proceeding consecutively from sample 1 to sample 3. The PHBV content among these three samples is identical, and the PLA content is nearly identical. Hence the decrease in stress is attributed to the increase of the plasticiser content from samples 1 to 3. However, from samples 2 to 3, the plasticiser content is constant. Hence it could be concluded that in sample 3 the ESA content act as a plasticiser. This could also indicate that sample 3 could contain excess ESA that has not reacted with

**Table 3.** Optimisation parameters.

| | Goal | Lower | Target | Upper | Weight | Importance |
|---|---|---|---|---|---|---|
| Elongation at break [%] | Maximum | 100 | 500 | 500 | 1 | 1 |
| Cost [NZD/kg] | Minimum | 10 | 10 | 15 | 1 | 1 |
| $\eta_e$ at $\gamma_a$ | Maximum | 1400 | 3660 | 3660 | 1 | 1 |

**Table 4.** Predicted optimal component compositions for a targeted response setting.

| Component | Percentage | Predicted response | Value | Desirability |
|---|---|---|---|---|
| PLA | 57.40 | Elongation at break [%] | 206.83 | 0.267076 |
| PHBV | 30.00 | Cost [NZD/kg] | 13.67 | 0.266246 |
| Plasticiser | 11.36 | $\eta_e$ at $\gamma_a$ | 2932.68 | 0.678175 |

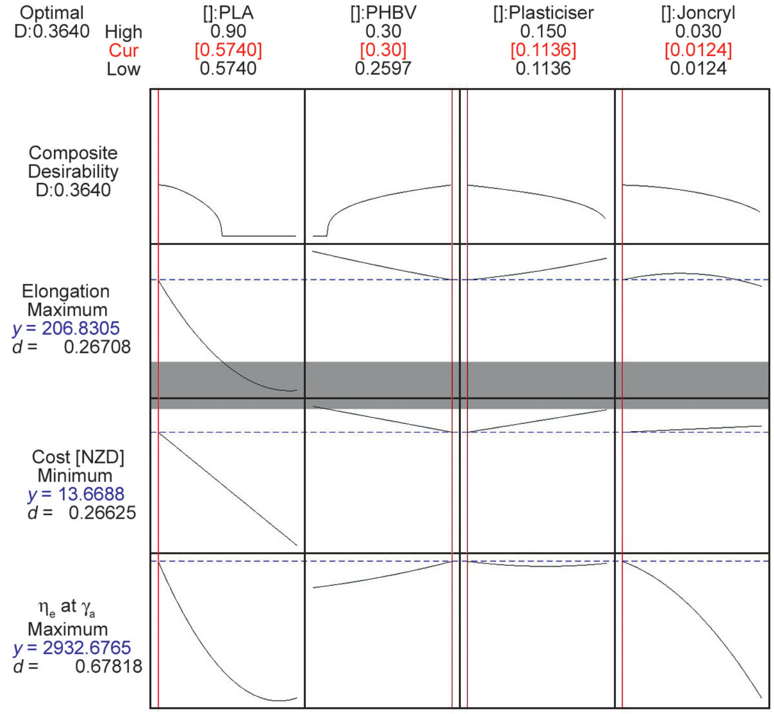

**Figure 8.** Response optimisation plot.

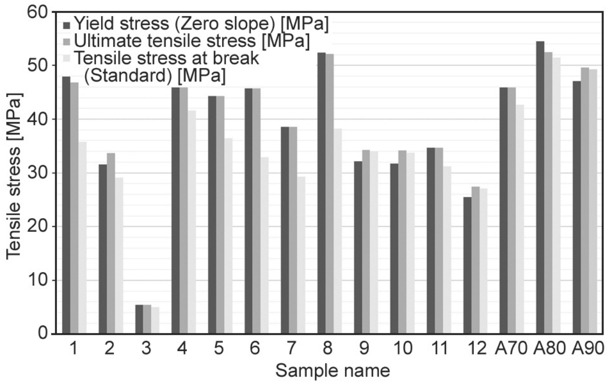

**Figure 9.** Tensile stress, yield, and ultimate tensile stress of the filament-like extruded samples.

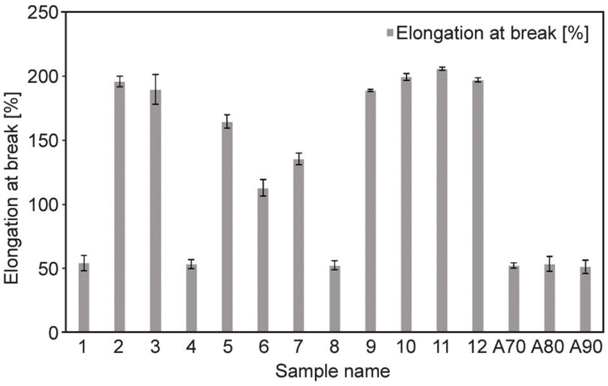

**Figure 10.** Elongation at break of the filament-like extruded samples.

the terminal hydroxyl and carboxylic acid groups in PLA and PHBV polymer chains. Samples 2 and 3 both have significantly higher percent elongation at breaks, corroborating the plasticising effect of TC and ESA.

From sample 4, the tensile stress properties are back to a 40 to 50 MPa range again, and then it declines as proceeds to sample 7. It is understandable that in sample 4, the lack of ESA [36] and the lower TC contents [11] leads to a more brittle blend, possessing a percent elongation at break of only 50% with high tensile stress properties among all samples. It is also interesting to see that sample 4 and sample 1 can withhold almost the same ultimate tensile stress (about 46 MPa) while containing completely different component proportions. This could be of interest in a practical application where cost optimisation is necessary. Sample 5, similar to sample 4 in polymer and plasticiser composition, has only the addition of ESA content. As discussed earlier, the excess (or unreacted) ESA content can act as a plasticiser in the blend, increasing the ductility while reducing the tensile stress of the compound relative to the sample 4 values.

Samples 6 and 7 possess equal contents of PLA and PHBV and varying contents of TC and ESA. In these two compounds, the PLA content is higher than samples 4 and 5 by around 20 to 25%, projecting a slightly different synergistic effect on their tensile properties. As a result, samples 6 and 7 have lower tensile stress than 4 and 5. Another characterisation of the blend that could be identified from the results can be seen in the contrasting results of samples 7 and 3. In sample 3, the tensile stress, ultimate tensile stress, and yield stress all have nearly the same value, whereas, in sample 7, the tensile stress sits about 25% lower on the stress axes than ultimate tensile and yield stress. This is indicative that sample 3, under axial stress, does not enter plastic deformation; hence the material experiences a continuous elastic stretch from the onset until the breaking point. However, samples 7 (as well as 4, 5, 6, and 8) experience plastic deformation, presenting different values of yield stress and tensile stress at break.

Sample 8 shows similar results to sample 4. They both have some of the highest tensile properties and low (about 50%) strain at break among all. These two samples have equal plasticiser and chain extenders and varying polymer contents. The higher PLA content explains the higher yield stress in sample 8. It also becomes apparent that sample 4 experiences a shorter elastic deformation than sample 8. There is not much compositional difference between sample 9 and sample 10. These compositions were mathematically generated to take account of all plausible interactive effects incurred by variation of composition content. Sample 9 has only 1% more PHBV content (less plasticiser content) in its composition. This slight material difference manifests its effect in a 10% increase in elongation at the break of sample 10.

zilar condition in comparison, except here, with the presence of an ESA chain extender. Sample 12 possessed 4% less PHBV content and was replaced by plasticiser. As a result, sample 12 have about 10 MPa lower tensile stress, ultimate, and yield stress than sample 10 and 9% lower strain at break. It could also be concluded that sample 12 experienced a lower plastic deformation than sample 11.

Samples A90, A80, and A70, contain no plasticiser nor chain extender and a PLA/PHBV ratio of 90/10, 80/20, and 70/30, respectively. The first noticeable result from these compositions is the higher values of tensile stress (in the 45 to 55 MPa region) and low elongation at break (in the 50% region) among all samples. The strain at break remains almost the same as proceeding consecutively from A70 to A90. This indicates that if no additives are used, the incorporation of even up to 30% PHBV content in a blend with PLA cannot reduce the rigidity of the blend and increase its ductility. The tensile strength properties show a nonlinear relationship between PHBV content and tensile strength; hence a synergistic effect is identified. The synergistic effect is manifested in sample A80 as it possesses a higher stress value than A70 and A90.

## 3.3. Thermal properties

The melting temperature of pristine PLA and PHBV used in the sample compositions were separately measured to be 150.2 and 175.1 °C, respectively. The lower melting temperature values of PLA explain the lower $T_m$ values of samples 1, 2, 3, 6, and 7, as these samples contain the largest contents of PLA. This applies to sample A90 as well. The rest of the samples have a $T_m$ in a narrow range of 165 to 172 °C, indicating the trivial effect of TC and ESA on the melting behaviour of the compounds.

As can be seen in Figure 11, a range of enthalpy-of-fusion values is obtained for the samples, indicating that a different crystalline structure is formed for each mixture composition. PLA has a slow crystallisation rate [37]. Therefore, when a sample containing PLA content goes through the manufacturing process and then cools down to environment temperature, its PLA content holds a lower $\Delta H_{fus}$ than the PLA material before the process. This is because the lactide polymers need a longer time to arrange and form crystal lamellae [38].

In this test, the thermal properties were calculated from the second heating cycle of the DSC thermographs. Therefore, PLA polymer contents had a narrow window to fully crystallise. The lower degrees of crystallinity and slow crystallisation rate results in the formation of shorter crystal structures in processed PLA compared to processed PHBV. This incurs lower enthalpy of fusion values. Therefore, this could be associated with the lower $\Delta H_{fus}$ values of samples 1, 7, 8, and A90 due to their high PLA contents. This trend is followed by samples 2, 6, and A80 for having proportionally higher PLA contents. It can also be deduced that the presence of a chain extender can result in the formation of new and larger crystal structures. This can be seen in comparing the enthalpy of fusion in sample 3 with samples 9 and 10. Sample 3 contains 16% higher PLA contents; hence it is expected to present lower $\Delta H_{fus}$ values than samples 9 and 10. But on the contrary, it has a higher value. This could be associated with the ESA content that is absent in samples 9 and 10 and present in sample 3. ESA is a multifunctional component that can react with the terminal carboxylic acid and hydroxyl groups in polyesters [39]. This extends the polymer chains, which increases the polymer's molecular mass. The molecular mass increase ensues under different conditions in molecular arrangement conditions when the polymer is being cooled. Therefore, a larger crystal structure could be formed.

All the glass transition temperatures ($T_g$) and the onset of crystallisation temperatures ($T_c$) in Figure 11 are indicative of PLA because PHBV has a $T_g$ and $T_c$ in the range of –10 to 20 °C [40], and these two polymers are immiscible. $T_g$ and $T_c$ have almost the same value in samples A70, A80, and A90. These samples contain only polymers and no additives. Compared with the rest of the samples, this means the addition of plasticiser and chain extender has a higher effect on changing the glass transition and crystallisation temperature of PLA. Samples 2, 3, 9, 10, 11, and 12

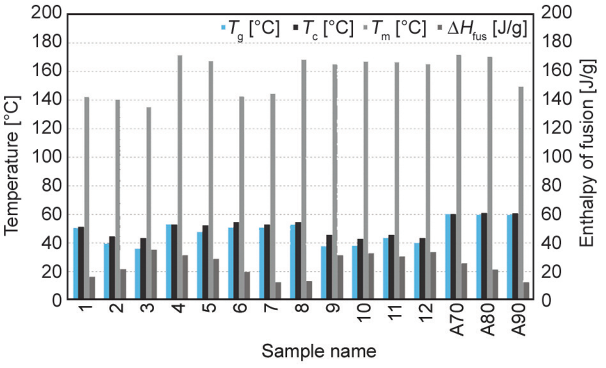

**Figure 11.** Thermal properties of the rod-like extruded samples obtained by differential scanning calorimetry.

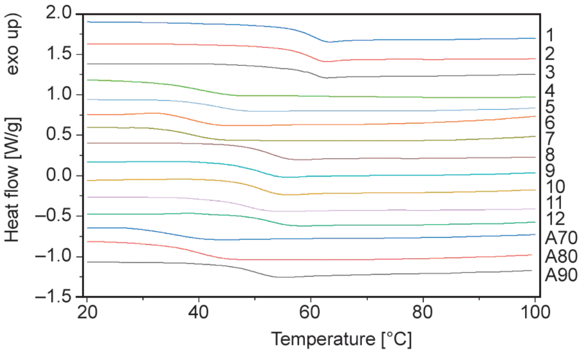

**Figure 12.** Thermograms of all samples from the second heating cycle obtained from DSC test.

specifically have the lowest $T_g$ and $T_c$ among all samples due to the highest plasticiser contents. Figure 12 shows the behaviour of thermograms near the glass transition region of each sample in their second heating cycle.

### 3.4. Rheology studies

Figure 13 depicts the rheology graphs obtained from the different blends. A non-Newtonian behaviour is observed for all samples; in other words, shear viscosity decreases with the increase of the shear rate. To further investigate the results, first, the pristine blends were assessed to identify whether the increase of PHBV content directly relates to the decrease of shear viscosity. As seen in Figure 13, it cannot be concluded that the increase of PHBV leads to a lower shear viscosity at any given shear rate value because the shear viscosity values of the A70 blend stand between the A80 and A90. The polymer chains typically stretch out in the machine direction during the processing stage due to the existing shear stress in the barrel and slide on one another. At this stage, the molecular structure and presence of additives or other blend components affect the chain mobility, hence affecting the shear viscosity of the blend. This synergistic effect has been reported by other researchers working with different grades of PLA and PHBV.

The synergistic rheological interaction between PLA and PHBV in a pristine blend (only at the PLA/PHBV ratio of 90/10, 80/20, and 70/30) is once more pronounced in Figure 14. This time it can be seen that with the increase in extensional strain rate, the A70 blend shows higher extensional viscosity values, specifically when the strain rate is in the $3.11\cdot10^7$ to $5.00\cdot10^8$ $s^{-1}$ range. This means that at identical processing conditions, the A70 blend at the given strain rate could provide a more stable bubble as extensional viscosity directly affect bubble stability in the blown film extrusion process. Generally, the higher the extensional viscosity, the more stable the bubble. However, for every polymer, extensional viscosity needs to reach a point from which the bubble could be formed (if the polymer is capable of being blown), and this value changes with the change in strain rate. If a blend's extensional viscosity is below the bubble formation viscosity, the bubble stability would not be a concern.

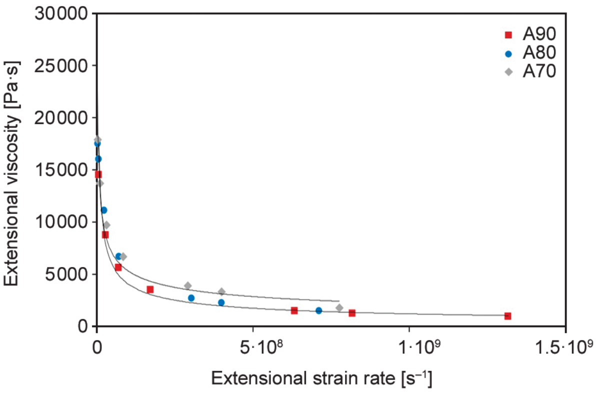

**Figure 14.** The extensional viscosity *vs*. extensional strain rate graph of pristine PLA/PHBV blends with a PLA to PHBV ratio of 90/10, 80/20, and 70/30.

One reason batches 2, 3, 10, and 12 were chosen to be blown to films was their highest values of extensional viscosities among all manufactured blends. Figure 15 provides a better understanding of the change in shear viscosity with the increase in shear rate. It can be seen that sample 3, followed closely by sample 12, presents the highest extensional viscosities among the blends along the shear rate axes. Sample 12 also offers the highest extensional viscosity at any given extensional strain rate (Figure 16). This was expected because both of these samples

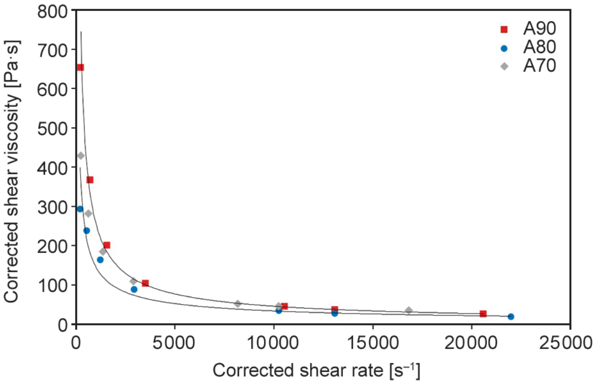

**Figure 13.** Comparison of shear thinning behaviour of pristine PLA/PHBV blends with a PLA to PHBV ratio of 90/10, 80/20, and 70/30.

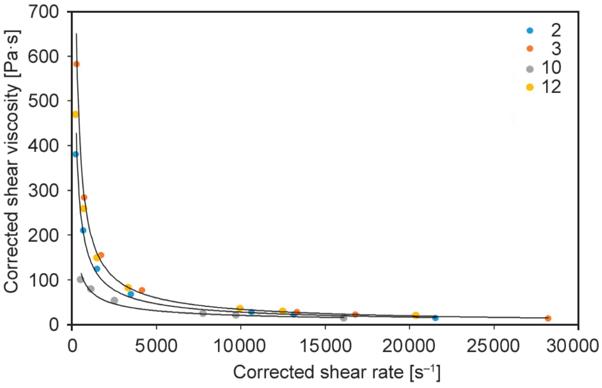

**Figure 15.** Comparison of the shear thinning behaviour of the chosen blends made into blown films.

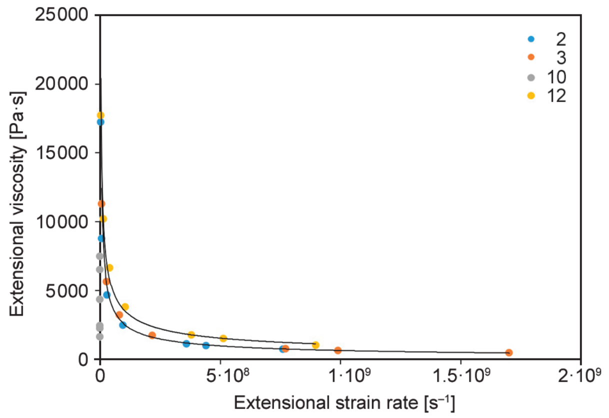

**Figure 16.** The extensional viscosity *vs*. extensional strain rate graph of the chosen blends that were made into blown film.

contained an ESA chain extender, contrary to the other two samples. The primary application of using chain extenders is to increase the melt viscosity in polymer blends. This, as explained earlier, is achieved by the reaction of the chain extender with the terminal –OH functional groups in PLA and PHBV polyesters, extending the chain length and hence restricting the molecular mobility of the polymers. Samples 3 and 12 have equal percent contents of ESA (chain extender) and TC (plasticiser), but sample 3 has lower PLA content. It can be concluded that in the manufacturing of blown films, in processing conditions, when the strain rate is below $1.0\cdot10^9$ s$^{-1}$, the blend with the lower PLA content could offer better bubble stability where the chain extender and plasticiser are equal proportions.

Batch 10 brings about some complexity to Figure 16. The only difference between batches 10 and 12 is ESA content. One can conclude that the lack of a chain extender in sample 10 results in plummeting extensional viscosity at very early values of strain rates. This is visible as the ηe values of sample 10 stack up on the $\eta_e = 0$. This is, of course, not the case, but it appears this way when the extensional strain rate is logarithmically plotted. This rheological behaviour could also mean that the increase of extensional viscosity is more dependent on the chain extender content (in this case, the presence and lack thereof of ESA) than the PLA content. This is deduced from the direct comparison of sample 2 and sample 10. PHBV polymer, due to having high degrees of crystallinity, has a low extensional viscosity at any given strain rate. Literature also shows that PHBV could not be blown into the film when not blended with another polymer with higher extensional viscosity and melt stress values. This means that PHBV percent content in a polymer blend acts as a bottleneck in the blown film extrusion process, given that other blend constituents have extensional viscosity and melt stress values higher than the point the bubble forms (depending on the processing temperature and screw speed).

To have a clear view of how the shear thinning behaviour of all mixture formulations compares with one another, a summary of the elongational viscosity vs. apparent shear rate of all samples is presented in Figure 17.

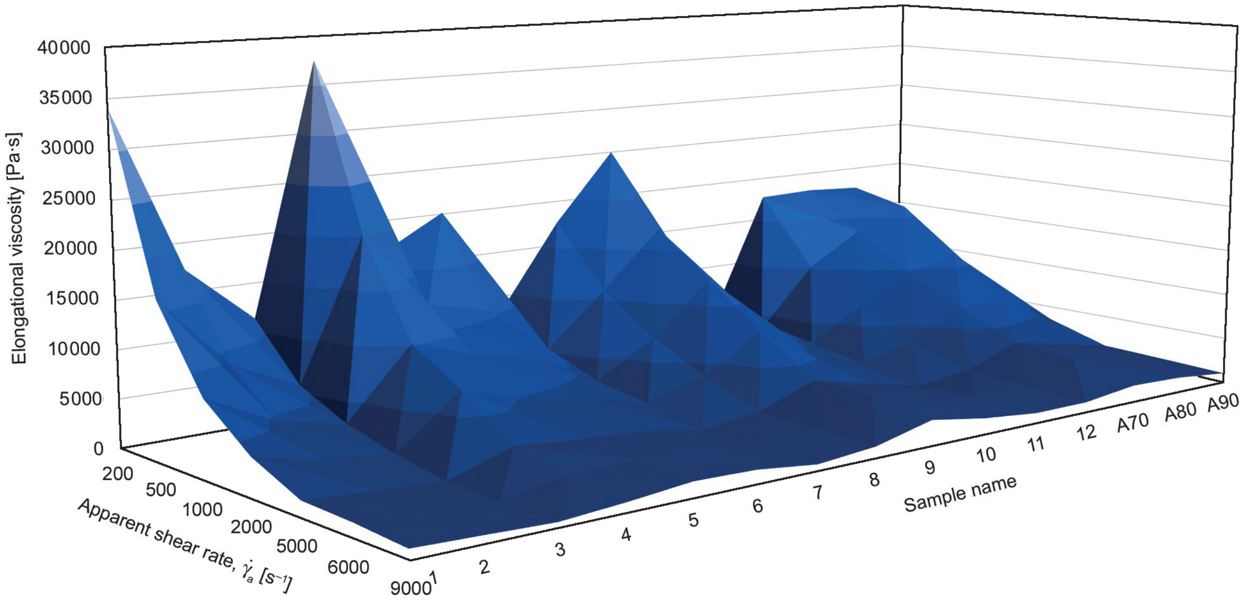

**Figure 17.** Summary of the differences in shear thinning behaviour of all blends compared with one another.

## 4. Conclusions

PLA and TC contents have the highest, and ESA content has the lowest total effectiveness in the blends. ESA content shows a nonlinear and interactive effect in responses as its linear content increase leads to the sudden rise and fall of crystallisation temperature, elongation at break, and tensile stress. The optimal values for the lowest cost and highest extension at break and the elongational viscosity were reached at PLA/PHBV/plasticiser/chain extender content of 0.574/0.3/0.113/0.012 wt%. The sample with the highest PLA content possessed the highest tensile stress. Also, the unreacted ESA content can act as a plasticiser in the blend, increasing the ductility and reducing the tensile strength of the compound. Finally, it cannot be simply concluded from rheology studies that the increase of PHBV leads to a lower shear viscosity at any given shear rate because the shear viscosity values of the A70 blend stood between the A80 and A90. This substantiates the synergistic effect of the PLA/PHBV blend in this range.

## Acknowledgements

The authors warmly acknowledge the financial support of Callaghan Innovation in New Zealand during the course of this research.

## References

[1] Dusselier M., van Wouwe P., Dewaele A., Jacobs P. A., Sels B. F.: Shape-selective zeolite catalysis for bioplastics production. Science, **349**, 78–80 (2015). https://doi.org/10.1126/science.aaa7169

[2] Penczek S., Szymanski R., Duda A., Baran J.: Living polymerization of cyclic esters–A route to (bio) degradable polymers. Influence of chain transfer to polymer on livingness. in 'Macromolecular symposia. Vol. 201, 261–270 (2003). https://doi.org/10.1002/masy.200351129

[3] Yu Y., Storti G., Morbidelli M.: Ring-opening polymerization of L,L-lactide: Kinetic and modeling study. Macromolecules, **42**, 8187–8197 (2009). https://doi.org/10.1021/ma901359x

[4] Li Z., Yang J., Loh X. J.: Polyhydroxyalkanoates: Opening doors for a sustainable future. NPG Asia Materials, **8**, e265 (2016). https://doi.org/10.1038/am.2016.48

[5] García-Campo M. J., Boronat T., Quiles-Carrillo L., Balart R., Montanes N.: Manufacturing and characterization of toughened poly(lactic acid) (PLA) formulations by ternary blends with biopolyesters. Polymers, **10**, 3 (2017). https://doi.org/10.3390/polym10010003

[6] Mendhulkar V. D., Shetye L. A.: Synthesis of biodegradable polymer polyhydroxyalkanoate (PHA) in cyanobacteria *Synechococcus elongates* under mixotrophic nitrogen- and phosphate-mediated stress conditions. Industrial Biotechnology, **13**, 85–93 (2017). https://doi.org/10.1089/ind.2016.0021

[7] Koller M., Salerno A., Tuffner P., Koinigg M., Böchzelt H., Schober S., Pieber S., Schnitzer H., Mittelbach M., Braunegg G.: Characteristics and potential of micro algal cultivation strategies: A review. Journal of Cleaner Production, **37**, 377–388 (2012). https://doi.org/10.1016/j.jclepro.2012.07.044

[8] Singh A. K., Sharma L., Mallick N., Mala J.: Progress and challenges in producing polyhydroxyalkanoate biopolymers from cyanobacteria. Journal of Applied Phycology, **29**, 1213–1232 (2017). https://doi.org/10.1007/s10811-016-1006-1

[9] Siracusa V., Rocculi P., Romani S., Dalla Rosa M.: Biodegradable polymers for food packaging: A review. Trends in Food Science Technology, **19**, 634–643 (2008). https://doi.org/10.1016/j.tifs.2008.07.003

[10] Fabra M. J., Lopez-Rubio A., Lagaron J. M.: Nanostructured interlayers of zein to improve the barrier properties of high barrier polyhydroxyalkanoates and other polyesters. Journal of Food Engineering, **127**, 1–9 (2014). https://doi.org/10.1016/j.jfoodeng.2013.11.022

[11] Crétois R., Follain N., Dargent E., Soulestin J., Bourbigot S., Marais S., Lebrun L.: Microstructure and barrier properties of PHBV/organoclays bionanocomposites. Journal of Membrane Science, **467**, 56–66 (2014). https://doi.org/10.1016/j.memsci.2014.05.015

[12] Jost V., Langowski H-C.: Effect of different plasticisers on the mechanical and barrier properties of extruded cast PHBV films. European Polymer Journal, **68**, 302–312 (2015). https://doi.org/10.1016/j.eurpolymj.2015.04.012

[13] Liu H., Zhang J.: Research progress in toughening modification of poly(lactic acid). Journal of Polymer Science part B: Polymer Physics, **49**, 1051–1083 (2011). https://doi.org/10.1002/polb.22283

[14] Acha B., Marcovich N., Reboredo M.: Lignin in jute fabric–polypropylene composites. Journal of Applied Polymer Science, **113**, 1480–1487 (2009). https://doi.org/10.1002/app.29999

[15] Al-Itry R., Lamnawar K., Maazouz A.: Biopolymer blends based on poly (lactic acid): Shear and elongation rheology/structure/blowing process relationships. Polymers, **7**, 939–962 (2015). https://doi.org/10.3390/polym7050939

[16] Tang W., Wang H., Tang J., Yuan H.: Polyoxymethylene/thermoplastic polyurethane blends compatibilized with multifunctional chain extender. Journal of Applied Polymer Science, **127**, 3033–3039 (2013). https://doi.org/10.1002/app.37538

[17] Chen X-H., Yu P., Kostromin S., Bronnikov S.: Minor-phase particles evolution in a polyethylene/ethylene–propylene copolymer (80/20) blend across mixing: Breakup and coalescence. Journal of Applied Polymer Science, **130**, 3421–3431 (2013).
https://doi.org/10.1002/app.39373

[18] Zuev V., Steinhoff B., Bronnikov S., Kothe H., Alig I.: Flow-induced size distribution and anisotropy of the minor phase droplets in a polypropylene/poly(ethylene-octene) copolymer blend: Interplay between break-up and coalescence. Polymer, **53**, 755–760 (2012).
https://doi.org/10.1016/j.polymer.2011.12.046

[19] Zuev V. V., Bronnikov S. V.: Statistical analysis of morphology of low density polyethylene/polyamide 6 blends with addition of organoclay and maleic anhydride-grafted polystyrene-*b*-poly(ethylene-*co*-butene-1)-*b*-polystyrene copolymer as compatibilizers. Journal of Macromolecular Science Part B, **51**, 1558–1565 (2012).
https://doi.org/10.1080/00222348.2012.656008

[20] Quiles-Carrillo L., Montanes N., Lagaron J. M., Balart R., Torres-Giner S.: *In situ* compatibilization of biopolymer ternary blends by reactive extrusion with low-functionality epoxy-based styrene–acrylic oligomer. Journal of Polymers and the Environment, **27**, 84–96 (2019).
https://doi.org/10.1007/s10924-018-1324-2

[21] Gérard T., Budtova T., Podshivalov A., Bronnikov S.: Polylactide/poly(hydroxybutyrate-*co*-hydroxyvalerate) blends: Morphology and mechanical properties. Express Polymer Letters, **8**, 609–617 (2014).
https://doi.org/10.3144/expresspolymlett.2014.64

[22] Li L., Huang W., Wang B., Wei W., Gu Q., Chen P.: Properties and structure of polylactide/poly(3-hydroxybutyrate-*co*-3-hydroxyvalerate) (PLA/PHBV) blend fibers. Polymer, **68**, 183–194 (2015).
https://doi.org/10.1016/j.polymer.2015.05.024

[23] Ma P., Spoelstra A. B., Schmit P., Lemstra P. J.: Toughening of poly(lactic acid) by poly(β-hydroxybutyrate-*co*-β-hydroxyvalerate) with high β-hydroxyvalerate content. European Polymer Journal, **49**, 1523–1531 (2013).
https://doi.org/10.1016/j.eurpolymj.2013.01.016

[24] Zhao H., Cui Z., Sun X., Turng L-S., Peng X.: Morphology and properties of injection molded solid and microcellular polylactic acid/polyhydroxybutyrate-valerate (PLA/PHBV) blends. Industrial and Engineering Chemistry Research, **52**, 2569–2581 (2013).
https://doi.org/10.1021/ie301573y

[25] Noda I., Satkowski M. M., Dowrey A. E., Marcott C.: Polymer alloys of Nodax copolymers and poly(lactic acid). Macromolecular Bioscience, **4**, 269–275 (2004).
https://doi.org/10.1002/mabi.200300093

[26] Nanda M. R., Misra M., Mohanty A. K.: The effects of process engineering on the performance of PLA and PHBV blends. Macromolecular Materials and Engineering, **296**, 719–728 (2011).
https://doi.org/10.1002/mame.201000417

[27] Han L., Han C., Zhang H., Chen S., Dong L.: Morphology and properties of biodegradable and biosourced polylactide blends with poly(3-hydroxybutyrate-*co*-4-hydroxybutyrate). Polymer Composites, **33**, 850–859 (2012).
https://doi.org/10.1002/pc.22213

[28] Liu Q., Wu C., Zhang H., Deng B.: Blends of polylactide and poly(3-hydroxybutyrate-*co*-3-hydroxyvalerate) with low content of hydroxyvalerate unit: Morphology, structure, and property. Journal of Applied Polymer Science, **132**, 42689 (2015).
https://doi.org/10.1002/app.42689

[29] Hedrick M. M., Wu F., Mohanty A. K., Misra M.: Morphology and performance relationship studies on biodegradable ternary blends of poly(3-hydroxybutyrate-*co*-3-hydroxyvalerate), polylactic acid, and polypropylene carbonate. RCS Advances, **10**, 44624–44632 (2020).
https://doi.org/10.1039/D0RA07485C

[30] Gong J., Qiang Z., Ren J.: *In situ* grafting approach for preparing PLA/PHBV degradable blends with improved mechanical properties. Polymer Bulletin, **79**, 9543–9562 (2021).
https://doi.org/10.1007/s00289-021-03958-6

[31] Yang M., Hu J., Xiong N., Xu B., Weng Y., Liu Y.: Preparation and properties of PLA/PHBV/PBAT blends 3D printing filament. Materials Research Express, **6**, 065401 (2019).
https://doi.org/10.1088/2053-1591/ab06cf

[32] Kanda G. S., Al-Qaradawi I., Luyt A. S.: Morphology and property changes in PLA/PHBV blends as function of blend composition. Journal of Polymer Research, **25**, 196 (2018).
https://doi.org/10.1007/s10965-018-1586-3

[33] Huang J-C., Leong K-S.: Shear viscosity, extensional viscosity, and die swell of polypropylene in capillary flow with pressure dependency. Journal of Applied Polymer Science, **84**, 1269–1276 (2002).
https://doi.org/10.1002/app.10466

[34] Bagley E.: End corrections in the capillary flow of polyethylene. Journal of Applied Physics, **28**, 624–627 (1957).
https://doi.org/10.1063/1.1722814

[35] Cogswell F.: Measuring the extensional rheology of polymer melts. Transactions of the Society of Rheology, **16**, 383–403 (1972).
https://doi.org/10.1122/1.549257

[36] Li H., Huneault M. A.: Effect of chain extension on the properties of PLA/TPS blends. Journal of Applied Polymer Science, **122**, 134–141 (2011).
https://doi.org/10.1002/app.33981

[37] Müller A., Ávila M., Saenz G., Salazar J.: Crystallization of PLA-based materials. in 'Poly(lactic acid) science and technology: Processing, properties, additives and applications' (eds.: Jiménez A., Peltzer M., Ruseckaite R.) The Royal Society of Chemistry, London, Vol. 12, 66–98 (2015).
https://doi.org/10.1039/9781782624806-00066

[38] Xu S., Li X., Sun C., Ni L., Xu W., Yuan W., Zheng Y., Yu C., Pan P.: Controllable crystallization and lamellar organization in nucleobase-functionalized supramolecular poly(lactic acid)s: Role of poly(lactic acid) stereostructure. Polymer, **232**, 124148 (2021).
https://doi.org/10.1016/j.polymer.2021.124148

[39] Coltelli M-B., Bertolini A., Aliotta L., Gigante V., Vannozzi A., Lazzeri A.: Chain extension of poly(lactic acid) (PLA)–based blends and composites containing bran with biobased compounds for controlling their processability and recyclability. Polymers, **13**, 3050 (2021).
https://doi.org/10.3390/polym13183050

[40] Mofokeng J. P., Luyt A. S.: Dynamic mechanical properties of PLA/PHBV, PLA/PCL, PHBV/PCL blends and their nanocomposites with $TiO_2$ as nanofiller. Thermochimica Acta, **613**, 41–53 (2015).
https://doi.org/10.1016/j.tca.2015.05.019